

# Supporting Information for

## Iron (III) Bromide Catalyzed Bromination of 2-*tert*-Butylpyrene and Corresponding Positions-Dependent Aryl-Functionalized Pyrene Derivatives

Xing Feng,<sup>a,b</sup> Jian-Yong Hu,<sup>b,c</sup> Hirotsugu Tomiyasu,<sup>b</sup> Zhu Tao,<sup>d</sup> Carl Redshaw,<sup>e</sup>  
Mark R.J. Elsegood,<sup>f</sup> Lynne Horsburgh,<sup>f</sup> Simon J. Teat,<sup>g</sup> Xian-Fu Wei,<sup>a</sup> and  
Takehiko Yamato<sup>\*b</sup>

<sup>a</sup> School of Printing and Packing Engineering, Beijing Institute of Graphic Communication, 1 Xinghua Avenue (Band Two), Daxing, Beijing 102600 P.R. China,

<sup>b</sup> Department of Applied Chemistry, Faculty of Science and Engineering, Saga University, Honjo-machi 1, Saga 840-8502 Japan. E-mail: yamatot@cc.saga-u.ac.jp

<sup>c</sup> Emergent Molecular Function Research Group, RIKEN Center for Emergent Matter Science (CEMS), Wako, Saitama 351-0198, Japan

<sup>d</sup> Key Laboratory of Macrocyclic and Supramolecular Chemistry of Guizhou Province, Guizhou University, Guiyang, Guizhou, 550025, P. R. China.

<sup>e</sup> Department of Chemistry, The University of Hull, Cottingham Road, Hull, Yorkshire, HU6 7RX, UK.

<sup>f</sup> Chemistry Department, Loughborough University, Loughborough, LE113TU, UK.

<sup>g</sup> ALS, Berkeley Lab, 1 Cyclotron Road, MS2-400, Berkeley, CA 94720, USA.

## Table of Contents

- 1 300 MHz  $^1\text{H}$ NMR spectrum of **1** and **2a**
- 2 300 MHz  $^1\text{H}$ NMR spectrum of **2b** and **2c**
- 3 300 MHz  $^1\text{H}$ NMR spectrum of **2d** and **2e**
- 4 300 MHz  $^1\text{H}$ NMR spectrum of **2f** and **3a**
- 5 300 MHz  $^1\text{H}$ NMR spectrum of **3b** and **3c**
- 6 300 MHz  $^1\text{H}$ NMR spectrum of **3b** and 400 MHz  $^1\text{H}$ NMR spectrum **3c**
- 7 300 MHz  $^1\text{H}$ NMR spectrum of **3e** and **3f**
- 8 100 MHz  $^{13}\text{C}$ NMR spectrum of **3a** and **3b**
- 9 100 MHz  $^{13}\text{C}$ NMR spectrum of **3c** and **3e**
- 10 75 MHz  $^{13}\text{C}$ NMR spectrum of **3f**
- 11 the key crystallographic data of **3**
- 12 Mechanism of bromination of 2-*tert*-butyl pyrene
- 13 Quantum Chemistry Computation

## Copy of NMR Spectra

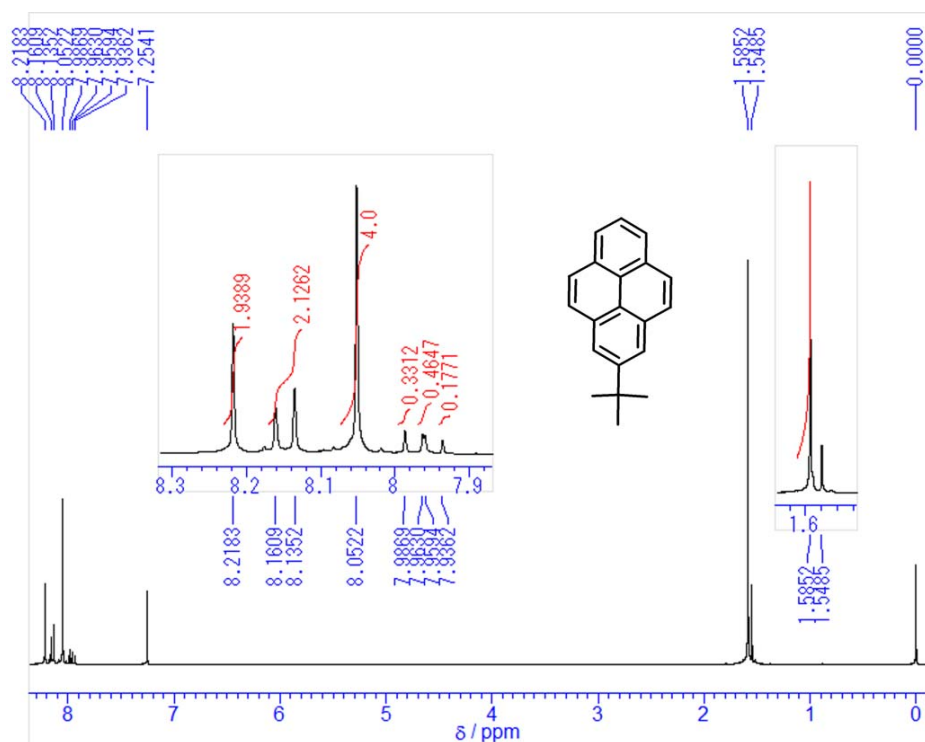


**Figure S1-1** <sup>1</sup>H-NMR spectrum (300 MHz, 293K, \* CDCl<sub>3</sub>) for **1** including an expansion of the aromatic region.

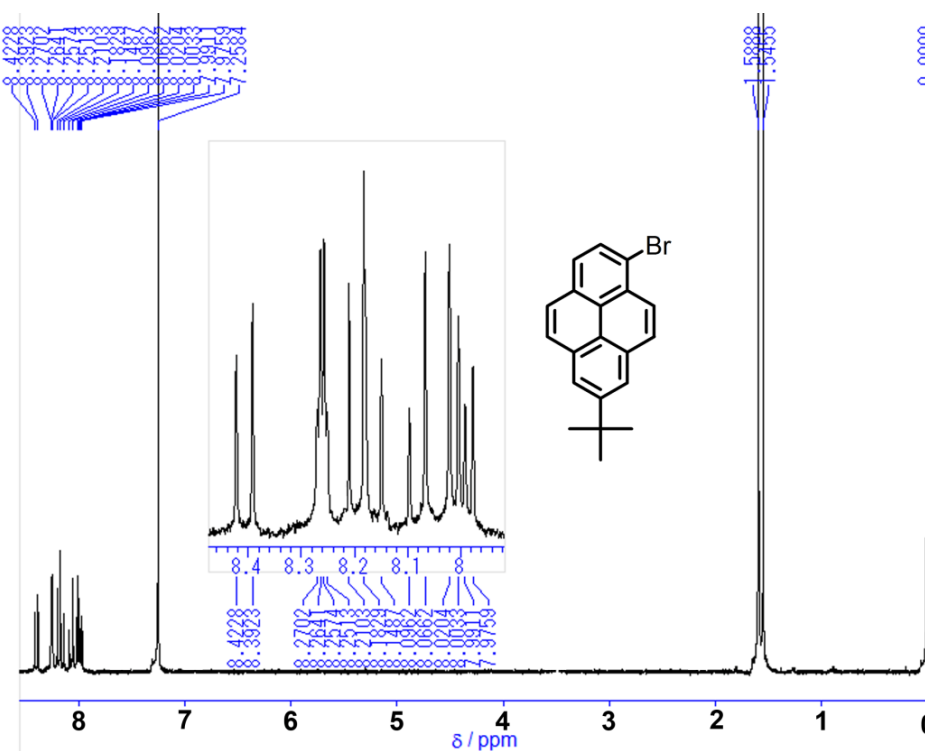


**Figure S1-2** <sup>1</sup>H-NMR spectrum (300 MHz, 293K, \* CDCl<sub>3</sub>) for **2a** including an expansion of the aromatic region.

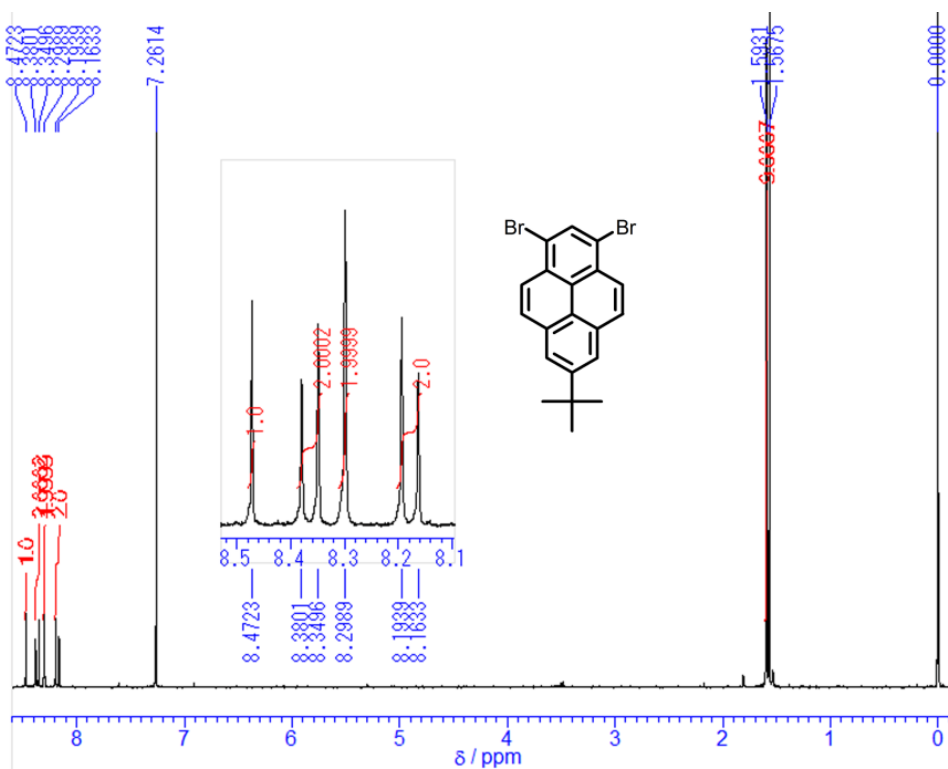


**Figure S1-3**  $^1\text{H-NMR}$  spectrum (300 MHz, 293K, \*  $\text{CDCl}_3$ ) for **2b** including an expansion of the aromatic region.

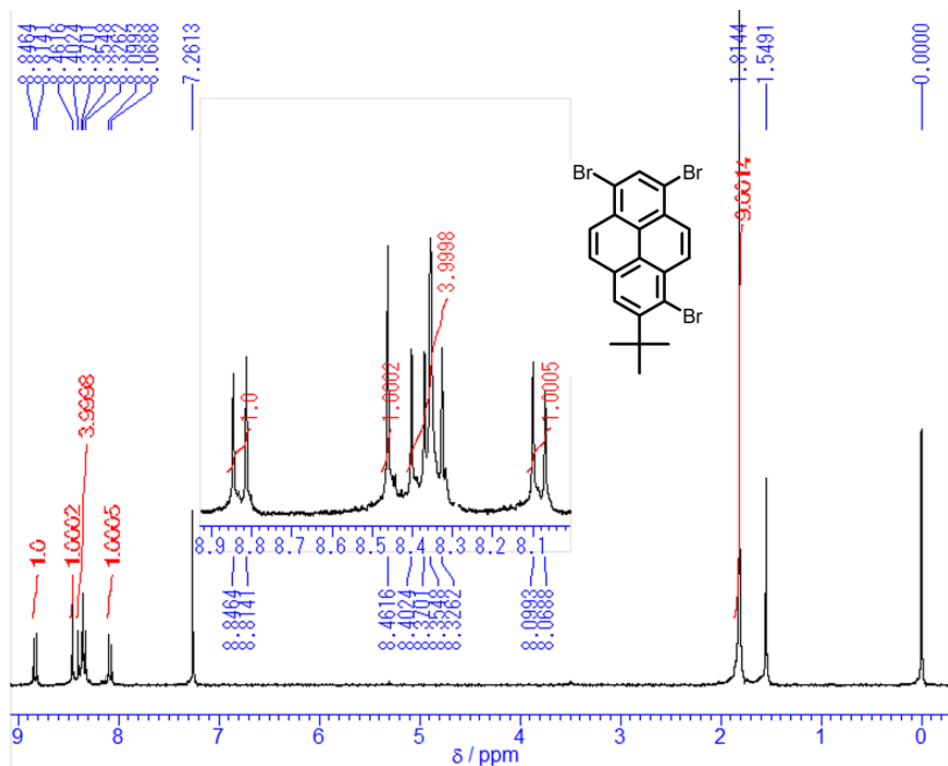


**Figure S1-4**  $^1\text{H-NMR}$  spectrum (300 MHz, 293K, \*  $\text{CDCl}_3$ ) for **2c** including an expansion of the aromatic region.

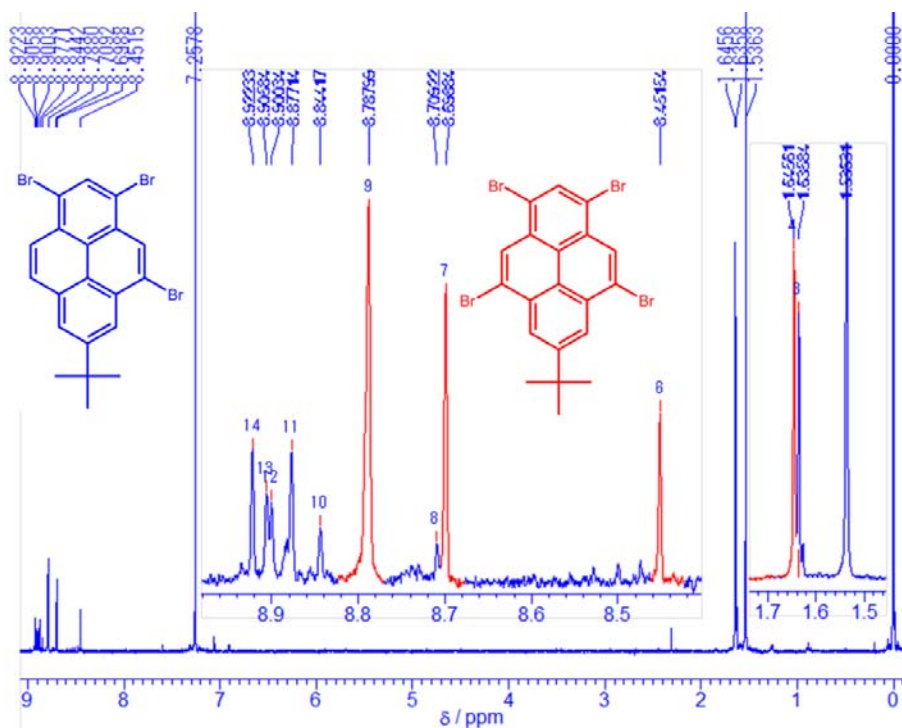


**Figure S1-5**  $^1\text{H-NMR}$  spectrum (300 MHz, 293K, \*  $\text{CDCl}_3$ ) of mixture **2d** and **2f** including an expansion of the aromatic region.

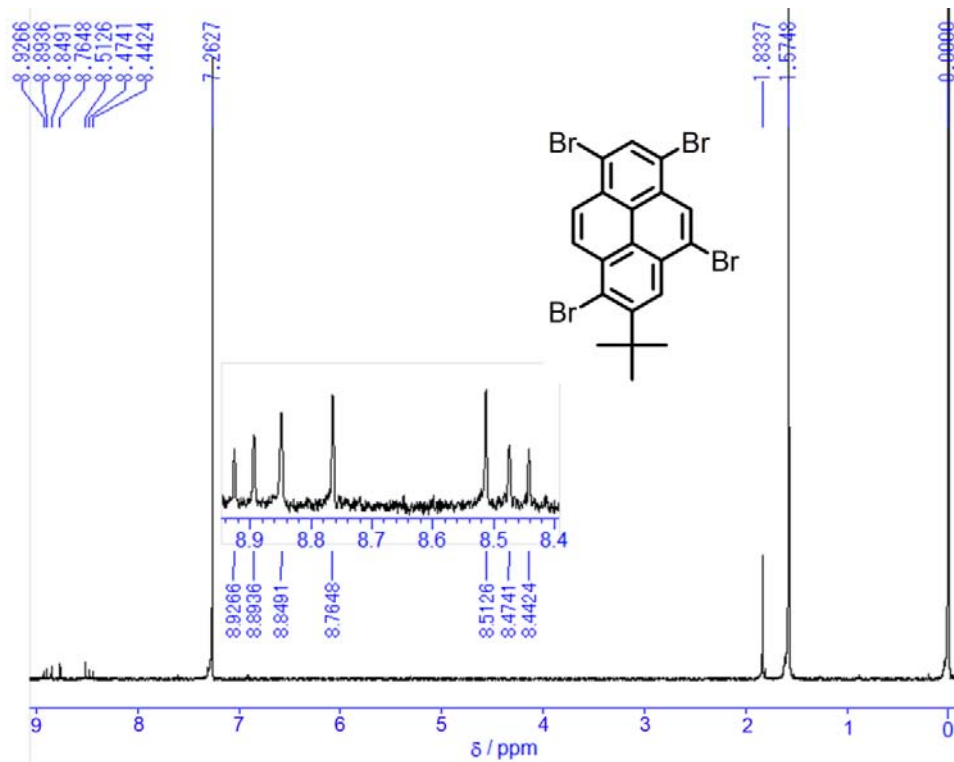


**Figure S1-6**  $^1\text{H-NMR}$  spectrum (300 MHz, 293K, \*  $\text{CDCl}_3$ ) for **2e** including an expansion of the aromatic region.

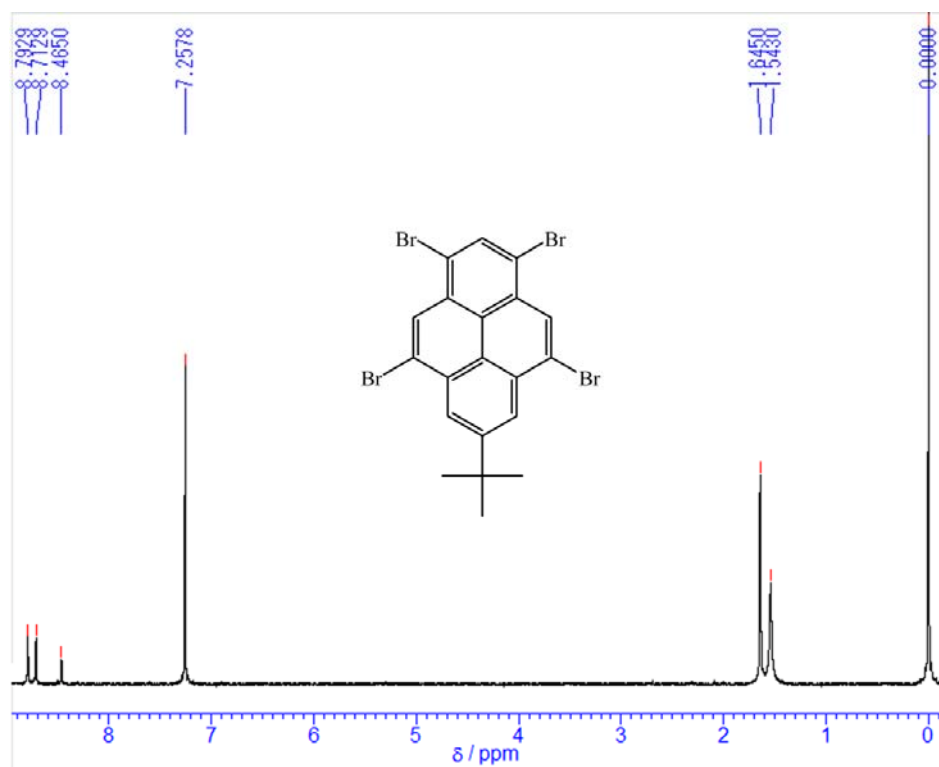


**Figure S1-14**  $^1\text{H-NMR}$  spectrum (300 MHz, 293K, \*  $\text{CDCl}_3$ ) for **3f**.

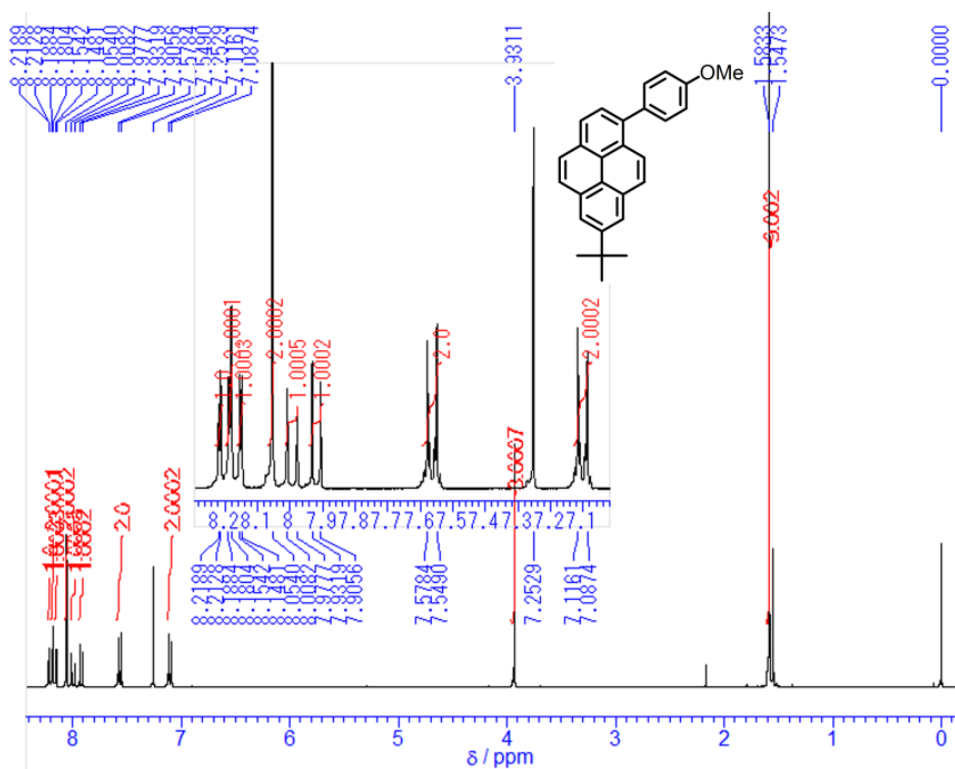


**Figure S1-8**  $^1\text{H-NMR}$  spectrum (300 MHz, 293K, \*  $\text{CDCl}_3$ ) for **3a** including an expansion of the aromatic region.

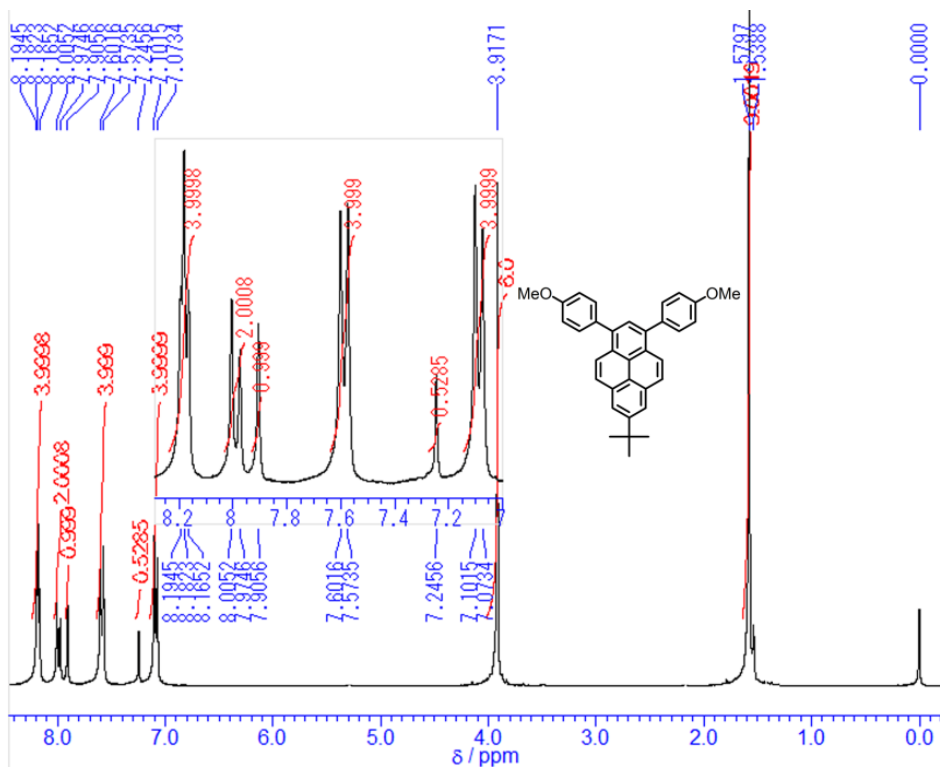


**Figure S1-9**  $^1\text{H-NMR}$  spectrum (300 MHz, 293K, \*  $\text{CDCl}_3$ ) for **3b** including an expansion of the aromatic region.

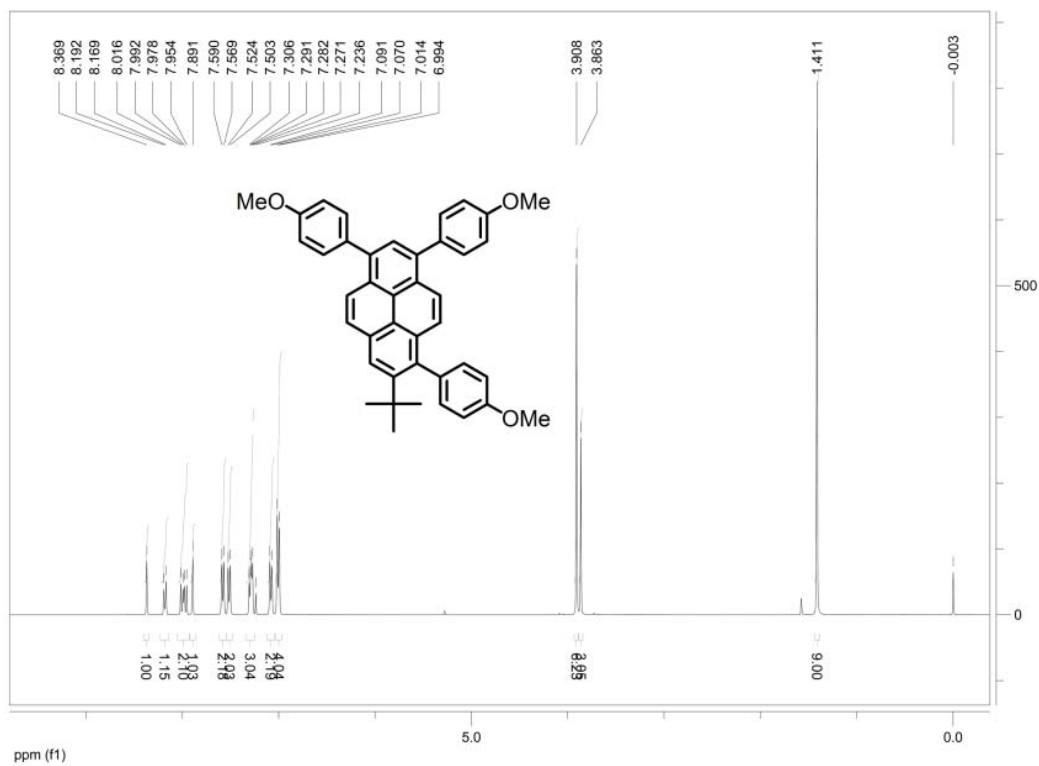


**Figure S1-10**  $^1\text{H-NMR}$  spectrum (400 MHz, 293K, \*  $\text{CDCl}_3$ ) for **3c**.





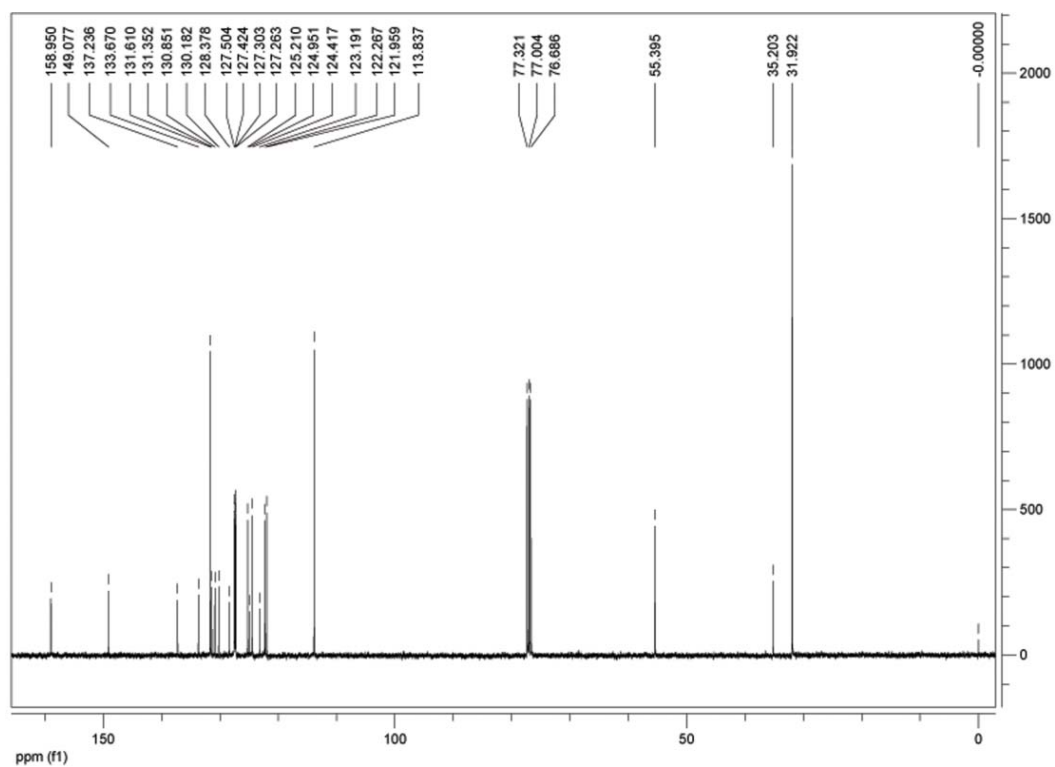


Figure S1-13  $^{13}\text{C}$ -NMR spectrum (100 MHz, 293K, \*  $\text{CDCl}_3$ ) for **3a**.

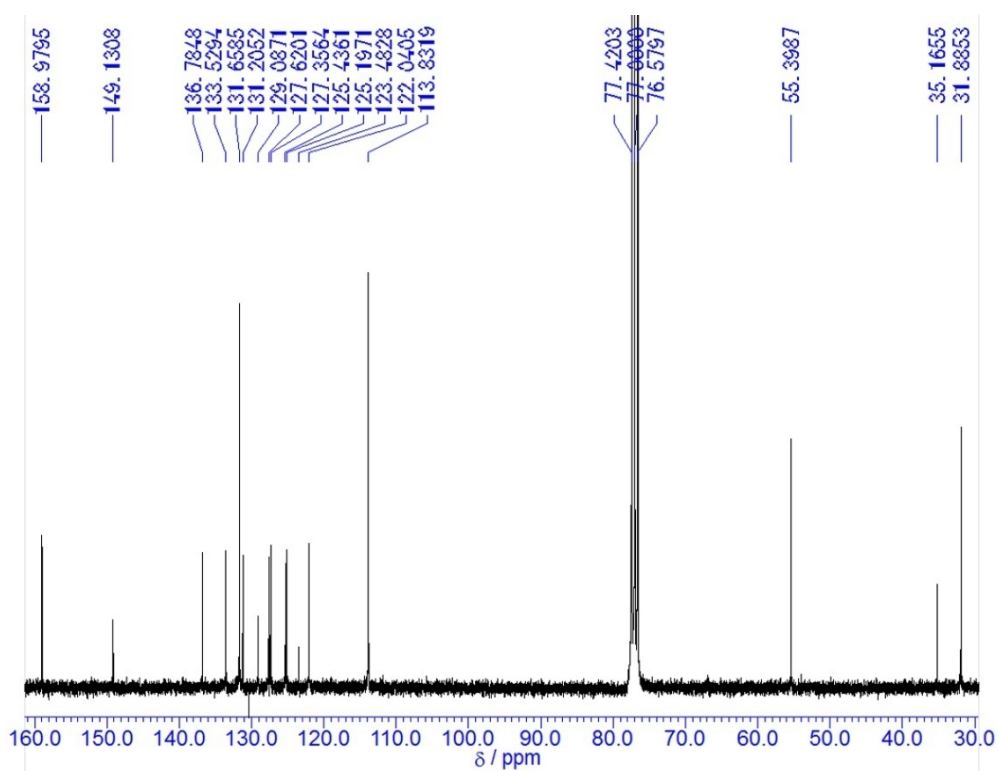


Figure S1-14  $^{13}\text{C}$ -NMR spectrum (75 MHz, 293K, \*  $\text{CDCl}_3$ ) for **3b**.

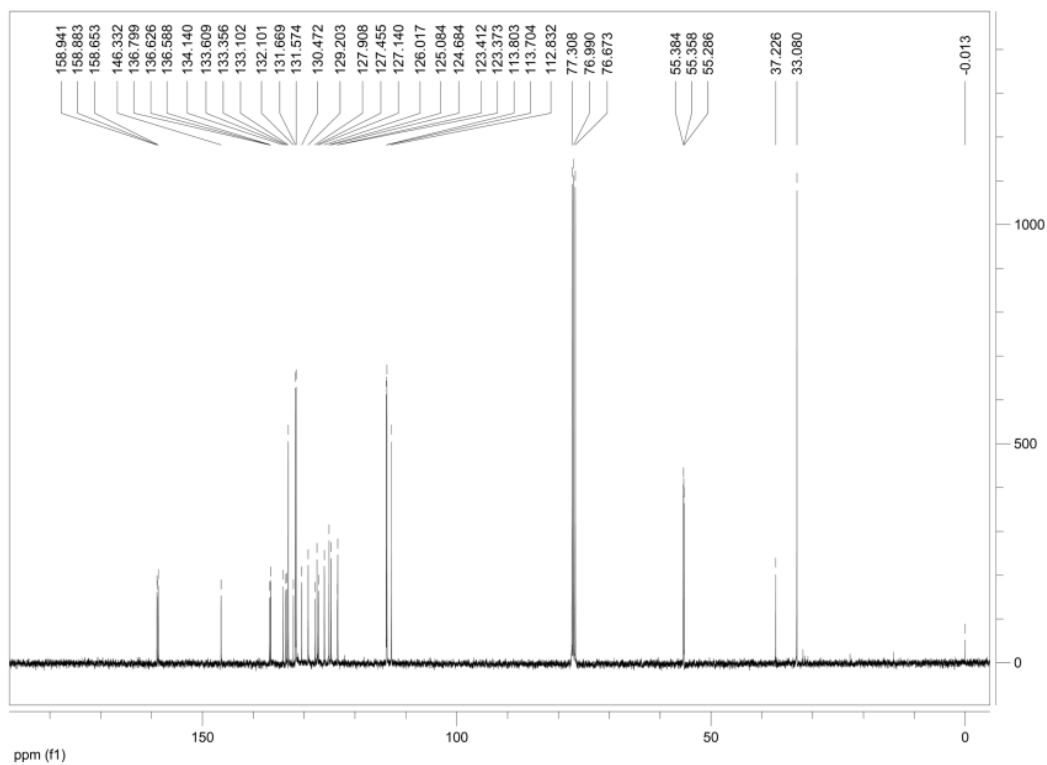


Figure S1-15  $^{13}\text{C}$ -NMR spectrum (100 MHz, 293K, \*  $\text{CDCl}_3$ ) for **3c**.

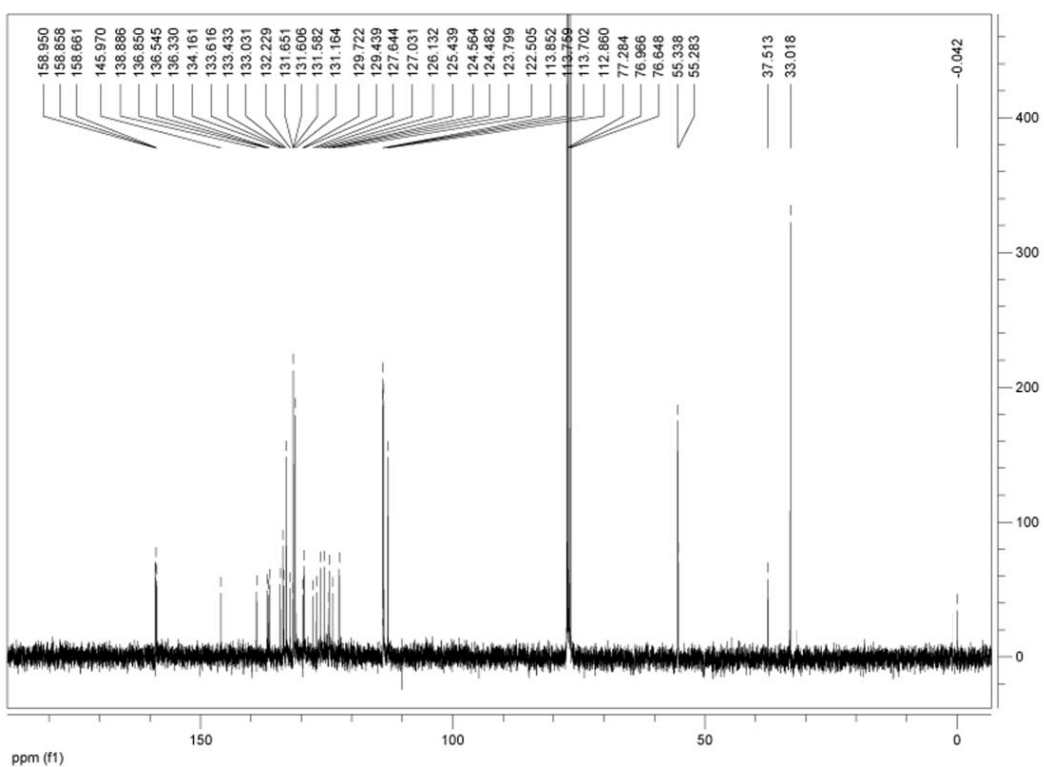
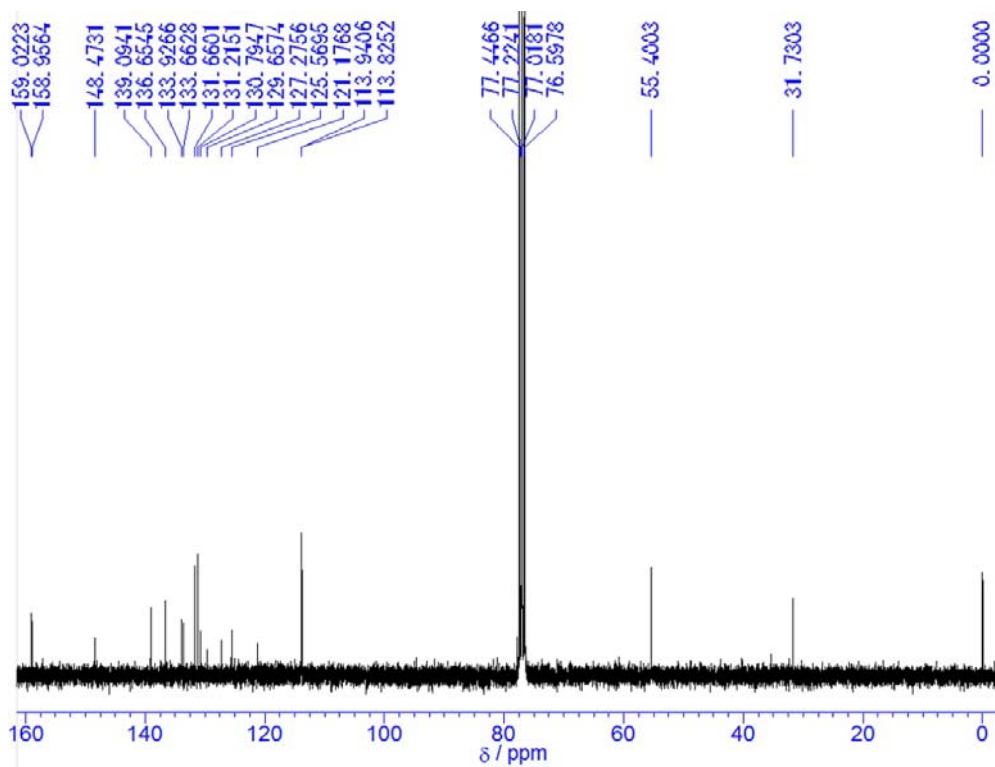


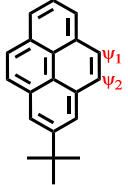
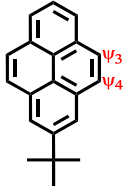
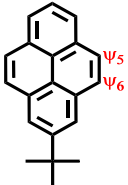
Figure S1-16  $^{13}\text{C}$ -NMR spectrum (100 MHz, 293K, \*  $\text{CDCl}_3$ ) for **3e**.



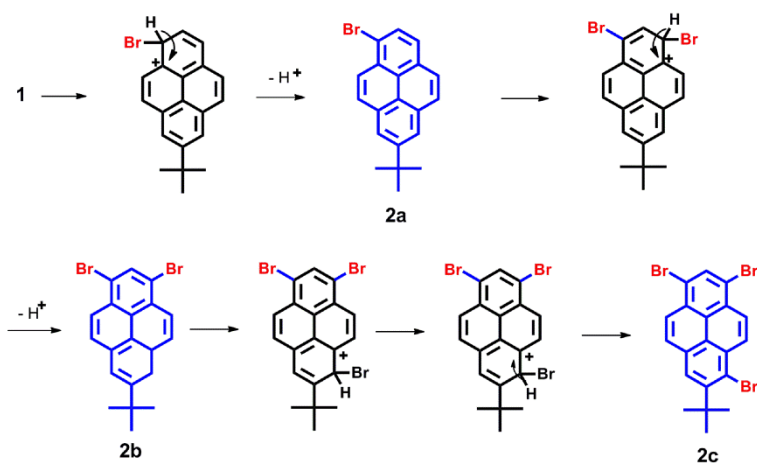
**Figure S1-17**  $^{13}\text{C}$ -NMR spectrum (75 MHz, 293K, \*  $\text{CDCl}_3$ ) for **3f**.

## Mechanism of bromination of 2-*tert*-butyl pyrene

Table S1 the ratio of benzenoid rings and double bonds<sup>[1]</sup>

Structure	Ratio	Coefficients	Nb	Ne
	$\psi_1 : \psi_2$	1.31	2	2
	$\psi_3 : \psi_4$	1.27	3	2
	$\psi_5 : \psi_6$	1.00	1	1

Nb=number of benzenoid rings ;Ne=number of exposed bonds



**Scheme S1** Possible regioselective bromination mechanism of **1**

[1] Moffitt, W. E.; Coulson, C. A. *Proc. Phys. Soc.*; **1948**, *60*, 309–315.

## X-Ray diffraction data

**Table S2** Summary of crystal data of pyrene derivatives **3**

Parameter	<b>3a</b>	<b>3b</b>	<b>3c</b>	<b>3d</b>	<b>3e</b>	<b>3f</b>
Empirical formula	C <sub>27</sub> H <sub>24</sub> O	C <sub>34</sub> H <sub>30</sub> O <sub>2</sub>	C <sub>41</sub> H <sub>36</sub> O <sub>3</sub>	C <sub>41</sub> H <sub>36</sub> O <sub>3</sub>	C <sub>48</sub> H <sub>42</sub> O <sub>4</sub>	C <sub>48</sub> H <sub>42</sub> O <sub>4</sub>
Formula weight [g mol <sup>-1</sup> ]	364.49	470.61	576.70	576.70	682.81	682.82
Crystal system	orthorhombic	monoclinic	Monoclinic	triclinic	monoclinic	triclinic
Space group	<i>P b c a</i>	<i>P2<sub>1</sub>/c</i>	<i>P2<sub>1</sub>/c</i>	<i>P -1</i>	<i>P2<sub>1</sub>/c</i>	<i>P-1</i>
<i>a</i> [Å]	34.643(4)	18.815(14)	9.136 (2)	10.299(6)	17.5703(6)	12.642(2)
<i>b</i> [Å]	11.0927(16)	15.629(11)	17.638 (4)	12.845(7)	8.8286(3)	12.960(2)
<i>c</i> [Å]	10.1811(13)	8.851(6)	19.524 (4)	13.482(12)	24.0368(9)	13.854(2)
$\alpha$ [°]	-	-	-	111.174(9)	-	86.048(2)°
$\beta$ [°]	-	103.255(9)	98.252 (4)°	103.142(10)	101.190(2)	67.354(2)°
$\gamma$ [°]	-	-	-	102.291(7)	-	60.942(2)°
Volume [Å <sup>3</sup> ]	3912.4(9)	2533(3)	3113.5 (12)	1531.8(19)	3657.7(2)	1811.4(5)
<i>Z</i>	8	4	4	2	4	2
Density, calcd [gm <sup>-3</sup> ]	1.237	1.234	1.230	1.250	1.240	1.252
Temperature [K]	113	123	150	296(2)	100(2)	150(2)
Unique reflns	3495	5722	7734	5187	73709	10122
Obsdreflns	2925	4734	6709	3075	13376	7260
Parameters	257	330	500	397	637	476
<i>R</i> <sub>int</sub>	0.0475	0.0640	0.034	0.0535	0.0404	0.0255
R[ <i>I</i> >2 $\sigma$ ( <i>I</i> )] <sup>a</sup>	0.0360	0.1034	0.048	0.0911	0.0441	0.0475
wR[ <i>I</i> >2 $\sigma$ ( <i>I</i> )] <sup>b</sup>	0.1041	0.3036	0.146	0.2649	0.1317	0.1413
GOF on F <sup>2</sup>	1.123	1.186	1.06	0.988	1.035	1.047

<sup>a</sup> Conventional R on F<sub>hkl</sub>:  $\Sigma||F_o| - |F_c||/\Sigma|F_o|$ . <sup>b</sup> Weighted R on |F<sub>hkl</sub>|<sup>2</sup>:  $\Sigma[w(F_o^2 - F_c^2)^2]/\Sigma[w(F_o^2)]^{1/2}$

# Quantum Chemistry Computation

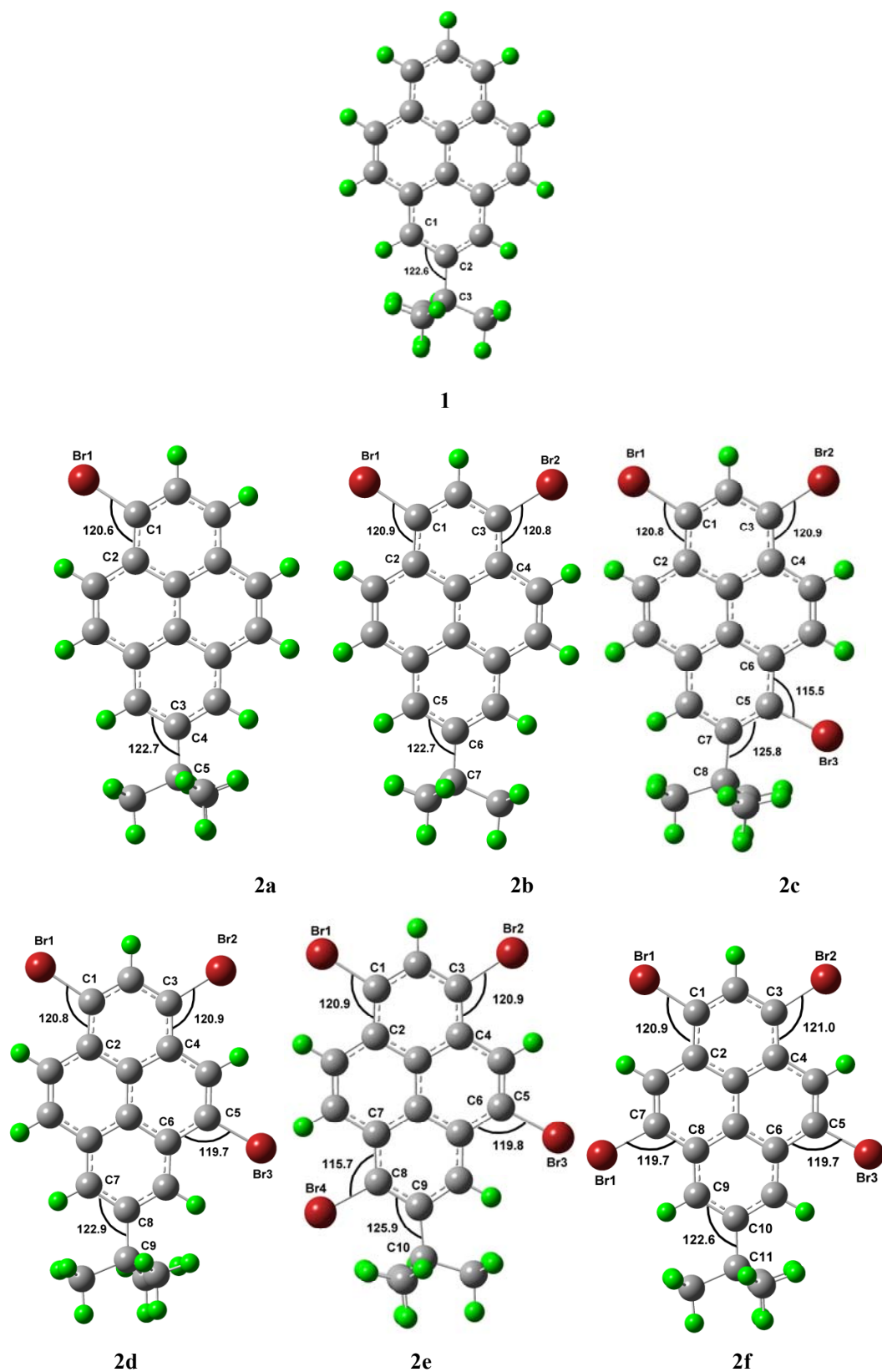


**Figure S2-2** Geometric structures of bromo-substituted pyrene **2** in the FeBr<sub>3</sub>-catalyzed reactions. The unit of angle is in °.

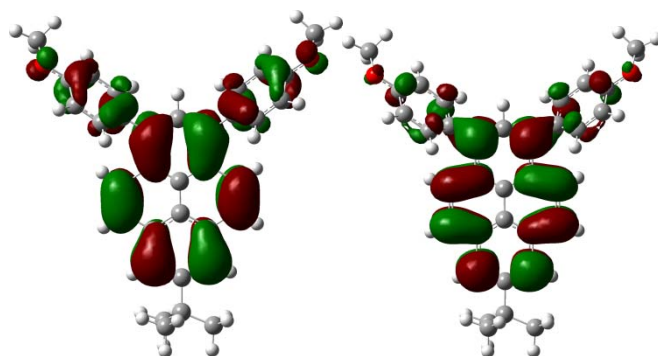


**Figure S3-1** Computed molecular orbital plots (B3LYP/6-31G\*) for **3b**: The left plots represent the HOMOs, and the right plots represent the LUMOs.

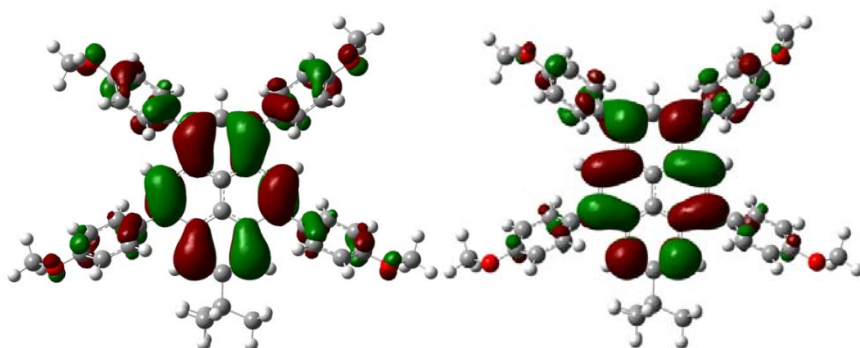


**Figure S3-2** Computed molecular orbital plots (B3LYP/6-31G\*) for **3f**: The left plots represent the HOMOs, and the right plots represent the LUMOs.

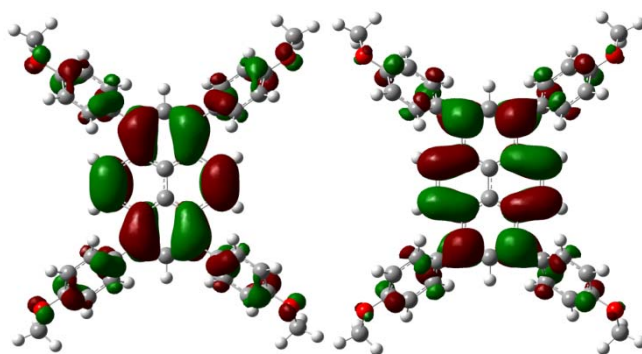


**Figure S3-3** Computed molecular orbital plots (B3LYP/6-31G\*) for **4**: The left plots represent the HOMOs, and the right plots represent the LUMOs.

Table S3. Physical and electrochemical properties of compounds **3**, **4** and **5**.

Compound	<u>LUMO</u> (eV) <sup>[a]</sup>	<u>LUMO</u> (eV) <sup>[b]</sup>	<u>E<sub>ox</sub><sup>1/2</sup></u> <sup>[c]</sup> (eV)	<u>E<sub>ox</sub><sup>onset</sup></u> <sup>[d]</sup> (eV)	<u>E<sub>ox</sub>(Fc)</u> <sup>onset</sup> <sup>[d]</sup> (eV)	<u>HOMO</u> (eV)	<u>HOMO-LUMO</u> $\Delta E$ (eV)
<b>3a</b>	-1.41	nd	nd	nd	nd	-5.06 <sup>[a]</sup> / nd	3.65 <sup>[a]</sup> / 3.30 <sup>[e]</sup>
<b>3b</b>	-1.41	-2.27	1.45	1.36	0.66	-4.93 / -5.44 <sup>[b]</sup>	3.51 / 3.17
<b>3c</b>	-1.39	-2.13	1.51	1.32	0.64	-4.84 / -5.06	3.45 / 3.13
<b>3d</b>	-1.39	nd	nd	nd	nd	-4.82 / nd	3.43 / nd
<b>3e</b>	-1.39	-2.33	1.64	1.59	0.65	-4.76 / -5.36	3.37 / 3.03
<b>3f</b>	-1.36	-2.34	1.67	1.61	0.65	-4.76 / -5.37	3.40 / 3.03
<b>4</b>	-1.47	nd	nd	nd	nd	-4.71 / nd	3.24 / 2.94
<b>5</b>	-1.22	nd	nd	nd	nd	-4.93 / nd	3.70 / 3.31

<sup>[a]</sup>DFT/B3LYP/6-31G\* using Gaussian, <sup>[b]</sup>HOMO and LUMO energy levels were calculated according to equations:  $-(4.8+E_{ox}^{onset})$  and  $LUMO = HOMO + E_g$ , <sup>[c]</sup> $E_{ox}^{1/2}$  is the half-wave potential of the oxidative waves, <sup>[d]</sup> $E_{ox}^{onset}$  is the onset potential of the first oxidative wave, with potentials *versus* Fc/Fc<sup>+</sup> couple. <sup>[e]</sup> $E_g$ : estimated from UV-vis absorption spectra in solution. nd. No determination.